International Journal of Science and Research (IJSR)
ISSN: 2319-7064
Impact Factor 2025: 7.089

GWO-Based MPPT and Intelligent Energy Management for a Hybrid PV-Wind-Fuel Cell System with Battery Storage Using a Dual-Phase Interleaved Boost Converter

Abobaker Mahdi Abobakr[1], Dr. Ch. Ravi Kumar[2]

[1]Research Scholar, Department of Electrical & Electronics Engineering, University College of Engineering, Acharya Nagarjuna University, Andhra Pradesh, India

[2]Assistant Professor, Department of Electrical & Electronics Engineering, University College of Engineering, Acharya Nagarjuna University, Andhra Pradesh, India

Abstract: ***This paper proposes a Grey Wolf Optimization (GWO)-based maximum power point tracking and energy-management framework for a DC-coupled hybrid renewable energy system comprising a photovoltaic (PV) array, a permanent-magnet synchronous-generator (PMSG)-based wind energy conversion system, a fuel-cell source and a battery energy storage system (BESS). The source architecture, dual-phase interleaved boost converter (IBC), bidirectional battery converter and nominal component values are retained from the supplied reference manuscripts. The two IBC phases operate with a 180° phase displacement and regulate the common DC link to 700 V. In the proposed extension, GWO searches for the duty-ratio or reference operating point that maximizes measured source power, while a supervisory GWO-based energy-management layer selects feasible source and storage power references subject to DC-link, battery state-of-charge (SOC), converter-current and source-power constraints. The fitness function is formulated to maximize renewable-energy utilization while penalizing DC-link voltage deviation, battery throughput and unnecessary charge/discharge reversals. The original manuscripts report an INC-controlled baseline and a converter comparison, including an approximately 700 V DC link and an average IBC efficiency of about 98.1%; these values are retained only as source-reported reference data.***

Keywords: Grey Wolf Optimization; maximum power point tracking; hybrid renewable energy system; photovoltaic; wind energy; battery energy storage; dual-phase interleaved boost converter; energy management; DC-link regulation

1. Introduction

The integration of complementary renewable sources is a practical route to improving the continuity and reliability of distributed DC power systems. PV generation is strongly affected by irradiance and cell temperature, wind generation varies with wind speed, and fuel-cell output is comparatively controllable but exhibits slower transient response. A BESS can absorb surplus generation and supply power during renewable-energy deficits. The supplied manuscripts describe this PV–wind–fuel-cell–battery arrangement and use a common 700 V DC link to couple the source-side converters and the load-side interface [1], [2].

The underlying studies apply Incremental Conductance (INC) MPPT, showing that a dual-phase IBC provides superior ripple and conversion efficiency relative to a standard single-phase boost converter. The present extension focuses on the control layer rather than changing the established power-stage architecture. GWO is introduced as a population-based optimizer inspired by the leadership hierarchy and hunting behaviour of grey wolves. The alpha, beta and delta candidates guide the remaining search agents, allowing the duty ratio or source operating reference to be updated without relying exclusively on a fixed perturbation step.

The main contributions proposed in this extension are: (i) a GWO-based MPPT controller for PV and wind source-side power extraction; (ii) a constrained GWO supervisory energy-management formulation for source dispatch and BESS power reference selection; (iii) coordinated integration with the existing two-phase IBC and bidirectional battery converter; and (iv) a common test protocol for comparing P&O, INC and GWO under changing environmental and load conditions. The contribution is a proposed control extension; performance improvements must be confirmed by executing the model and are not assumed in advance.

2. System Configuration and Design Specifications

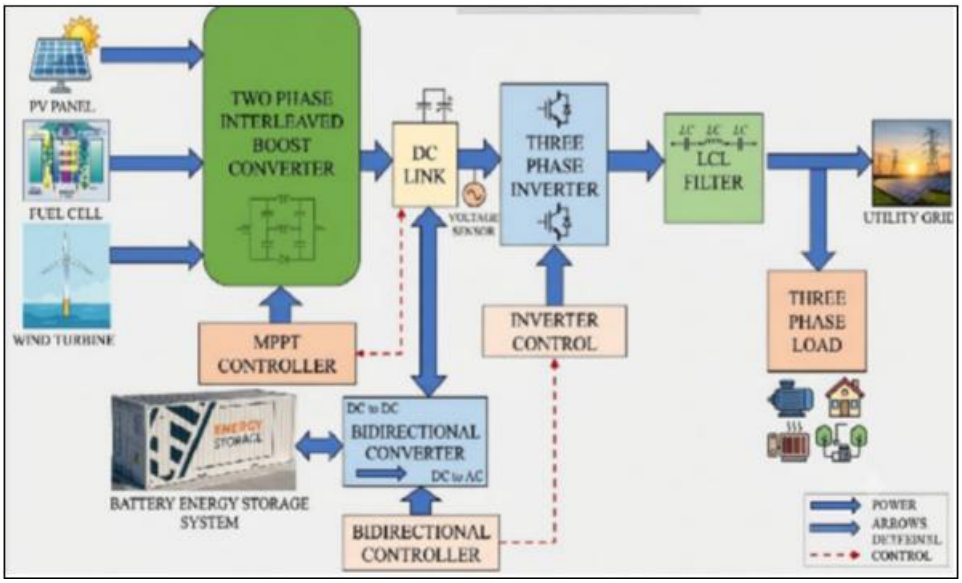


Figure 1: System Architecture of Grid Tied Hybrid System

The system is DC coupled. The PV array, rectified PMSG wind subsystem and fuel-cell source feed the high-voltage DC bus through source-side boost-converter interfaces. Each renewable-source interface uses two interleaved phases, with the second gate signal displaced by 180° from the first. The BESS is connected to the DC link through a bidirectional DC–DC converter. During surplus generation, the converter operates in buck/charging mode; during a generation deficit, it operates in boost/discharging mode. The source manuscripts also describe a grid-tied inverter, PLL, SVPWM and LCL filter. These may be retained if the study evaluates AC-side power quality; the core GWO MPPT and DC-side EMS evaluation can be performed at the DC link.

Parameter	Value reported in supplied source	Use in extension
PV power	100.7 kW at 1000 W/m² and 25 °C; about 120 kW at 1200 W/m²; about 50 kW at 500 W/m²	PV source rating / operating-point reference
Wind subsystem	80 kW mechanical/electrical output (as stated in source)	Wind source nominal reference
Fuel cell	120.4 kW rated output	Dispatchable source reference
BESS	108 kW; initial SOC = 50%	Storage power rating and initial condition
Battery nominal voltage/current	360 V / 300 A	Bidirectional converter reference
DC link	700 V nominal; 300 kW; 3061 µF reported	Voltage-control reference
Dual-phase IBC	Vin = 275–450 V; Vout = 700 V; L1 = L2 = 5 mH; Co = 12000 µF; fs = 20 kHz	Source-side converter design
Bidirectional converter	L = 20 mH; fs = 20 kHz; ΔIL = 30 A; ΔVC = 1.8 V; C = 0.625 µF reported	Battery interface reference; verify capacitor sizing before implementation

3. Mathematical model

3.1 PV source

The instantaneous PV output power is calculated from measured terminal voltage and current:

$$P_{PV}(t) = V_{PV}(t) \times I_{PV}(t).$$

For a PV array, the maximum-power point is the operating point at which the product V_{PV} IPV is maximized for the current irradiance and cell temperature. A detailed model should use the single-diode PV equation with module-specific series resistance, shunt resistance, photocurrent, diode saturation current and temperature coefficients. Those module-level parameters are not present in the supplied manuscripts and must be taken from the actual Simulink PV block or module datasheet.

3.2 Wind source

The system utilizes a wind energy conversion configuration where a wind turbine drives a Permanent Magnet Synchronous Generator (PMSG). The variable-frequency AC generated by the PMSG is rectified to DC before reaching the DC–DC conversion stage to facilitate stable power control.

The mechanical power extracted from the wind is governed by the standard aerodynamic formula:

$$P_w = \frac{1}{2} \rho A C_p(\lambda, \beta) u_w^3$$

- r is the air density, and A is the blade swept area πR^2
- U_w represents the upstream wind speed, with extracted power scaling with its cube (u).
- C (|, b) is the aerodynamic power coefficient (rotor efficiency), which is non-linearly dependent on the tip-speed ratio and the blade pitch angle b.

3.3 Fuel Cell and Battery

The fuel cell supplies a comparatively smooth controllable DC contribution. Its rated output is reported as 120.4 kW.

The BESS is rated at 108 kW with an initial SOC of 50%. A simplified SOC update for simulation is:
$SOC(k+1) = SOC(k) - [P_{bat}(k)\,\Delta t / E_{bat}] \times 100\%,$

where the sign convention must be fixed consistently (positive P_bat may be defined as battery discharge), E_bat is the usable battery energy in kWh, and charge/discharge efficiencies should be included in a detailed model. Battery energy capacity, SOC limits and charge/discharge efficiencies are not explicitly established by the supplied excerpts and must be entered from the actual battery model.

3.4 Dual-phase interleaved boost converter

The ideal boost conversion relationship for either phase is $V_o = V_{in}/(1-D)$. For N interleaved phases, the average inductor current per phase is $I_{L,avg} = I_o/[(1-D)N]$. The source design uses N = 2 and a 180° phase displacement. The two phase currents combine at the output, and their ripple components partially cancel. Both phases operate at the same switching frequency; the effective ripple frequency at the combined input/output is twice the individual switching frequency.

The duty ratio is constrained to a safe interval, $D_{min} \le D \le D_{max}$, selected according to the actual source voltage range, device ratings and continuous-conduction operating limits. GWO should generate a common duty reference or a source-specific reference that is subsequently mapped to two PWM signals with a 180° phase shift. GWO must not directly replace the fast current/voltage protection loops.

3.5 DC-link and power balance

The DC-link power balance can be represented as:
$P_{PV} + P_w + P_{FC} + P_{bat} = P_{load} + P_{loss} + d(\tfrac{1}{2} C_{dc} V_{dc}^2)/dt.$
The control objective is to keep V_{dc} close to 700 V while satisfying source and battery constraints. A DC-link PI regulator or equivalent fast feedback loop should remain responsible for rapid voltage correction; the GWO supervisory layer supplies feasible power references at a slower update rate.

4. Proposed GWO-Based Control Strategy

4.1 Grey Wolf Optimization

Each search agent represents a candidate control variable, such as converter duty ratio D or a vector of dispatch references. The best three agents are designated alpha, beta and delta. For a candidate position X and leader position X_leader, the standard GWO update is:
$A = 2\,a\,r_1 - a;\;\; C = 2\,r_2;\;\; D_{leader} = |C\,X_{leader} - X|;\;\; X_{leader,new} = X_{leader} - A\,D_{leader}.$

The parameter a decreases linearly from 2 to 0 over the maximum iteration count. The updated position is obtained by averaging the three leader-guided positions. Candidate values are clipped to the permitted control bounds. In MPPT, the fitness is the negative measured source power, so minimizing fitness maximizes extracted power.

4.2 GWO-based MPPT

At each MPPT update, the controller obtains source voltage and current and evaluates P = VI. A population of duty-ratio candidates is evaluated using the plant response or a validated source/converter model. The alpha candidate provides the duty-ratio reference after the prescribed iterations. The duty command is passed through rate limiting and saturation, then applied to the two IBC phases with a 180° shift. A practical implementation should use a fast inner converter controller and run GWO at a slower supervisory sampling rate to avoid requiring a full population of switching simulations at every PWM period.

For a PV subsystem, the MPPT fitness can be written as $J_{MPPT}(D) = -P_{PV}(D)$. For wind, the objective may maximize rectified electrical power or turbine mechanical power, depending on the controlled variable. The optimizer should be reset or reinitialized when a large environmental change is detected, while avoiding unnecessary restarts during steady operation.

4.3 GWO-assisted energy management

The EMS optimizer selects a dispatch vector u = [P_{PV}*, P_w*, P_{FC}*, P_{bat}*] or a reduced vector of controllable references. PV and wind are normally operated at their available maximum-power points unless curtailment is required to respect DC-link, converter or battery constraints. Fuel-cell power is constrained by its rated value and ramp-rate limit. Battery power is constrained by its 108 kW rating, SOC limits and charge/discharge current limits.

A proposed multi-objective fitness function is:
$J_{EMS} = w_1(P_{load} - P_{supplied})^2 + w_2(V_{dc} - 700)^2 + w_3(P_{bat})^2 + w_4|\Delta P_{bat}| + w_5\,Penalty_constraints.$

Here $P_{supplied}$ is the net power delivered to the DC link, $w_1 \ldots w_5$ are non-negative weights, and Penalty_constraints imposes a large cost for SOC, current, voltage, power or ramp-rate violations. The P_{bat}^2 and $\Delta P_{bat}|$ terms discourage unnecessary battery throughput and rapid charge/discharge reversals. Weight values must be tuned and reported transparently. The fast bidirectional-converter current loop and DC-link voltage loop remain active beneath the EMS.

4.4 Control Hierarchy

Layer	Controller	Typical role
Source level	GWO MPPT	Find PV/wind maximum-power operating point
Converter level	PWM + current/voltage PI loops	Regulate inductor current, enforce duty limits, generate 180° phase-shifted gates
Storage level	Bidirectional converter PI loops	Track charge/discharge current references with SOC and current protection
Supervisory level	GWO-based EMS	Allocate source and battery power references; minimize voltage error and battery cycling
Protection level	Limiters and interlocks	Over/under-voltage, over-current, SOC limits, fuel-cell ramp limits and anti-windup

5. Results and Discussion

A hybrid system with a grid connection that uses renewable energy sources PV, wind turbine, fuel cell, and battery energy storage system (BESS) all together and connected via an interleaved boost converter was created and MATLAB/ Simulink simulated in order to check the system performance for different dynamic and steady-state conditions. This system's main goal is to keep a continuous DC-link voltage of 700 V, while the three-phase inverter with an LCL filter connected to the grid takes care of the power flow, thus mainly eliminating harmonic distortions. The hybrid configuration was tested under three distinct operating scenarios:

1) Peak Solar and Low Wind Availability: irradiance (1200 W/m²) and wind speed (10 m/s), fuel cell compensates.
2) High Solar–Wind Generation: irradiance (1000 W/m²) and wind speed (12 m/s), fuel cell operates at nominal mode.
3) Low Solar–High Wind Generation: irradiance (500 W/m²) and wind speed (14 m/s), fuel cell compensates and BESS discharges.

Power Sources output under the varying conditions

The Solar PV System characteristics, PV Voltage, PV Current and PV Power under the varying conditions are shown in the below

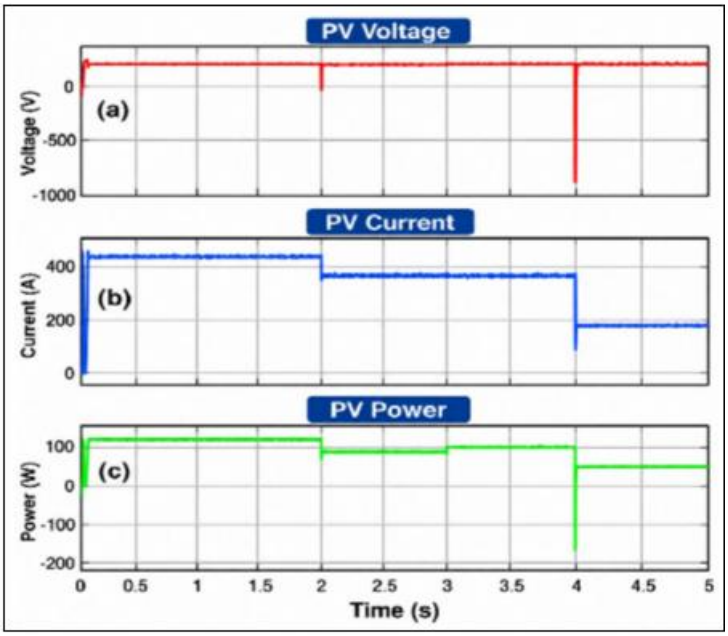


Figure 5: a) PV Voltage b) PV Current and c) PV Power

The Wind System characteristics, Wind Voltage, Wind Current and Wind Power under the varying conditions are shown in the below Fig.6

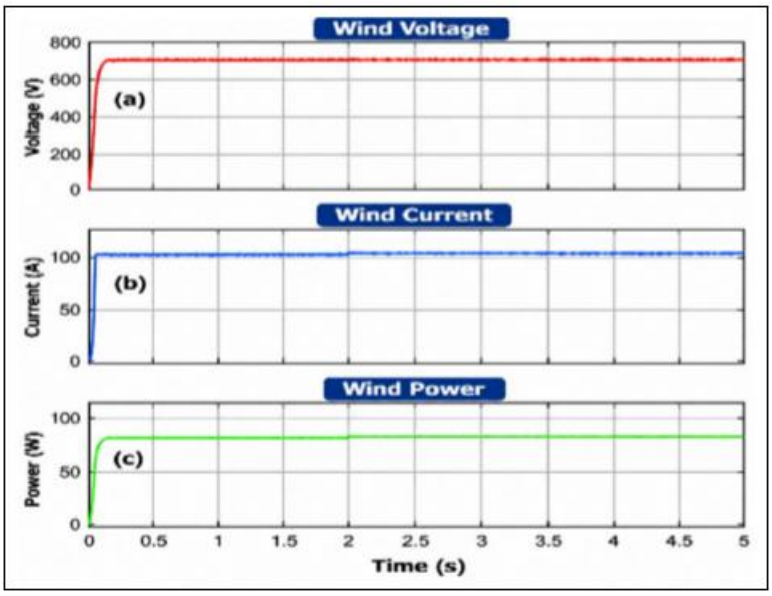


Figure 6: a) Wind Voltage, b) Wind Current and c) Wind Power

The Fuel Cell System, Fuel Cell Voltage, Fuel Cell Current and Fuel Cell Power under the varying conditions are shown in Fig.7

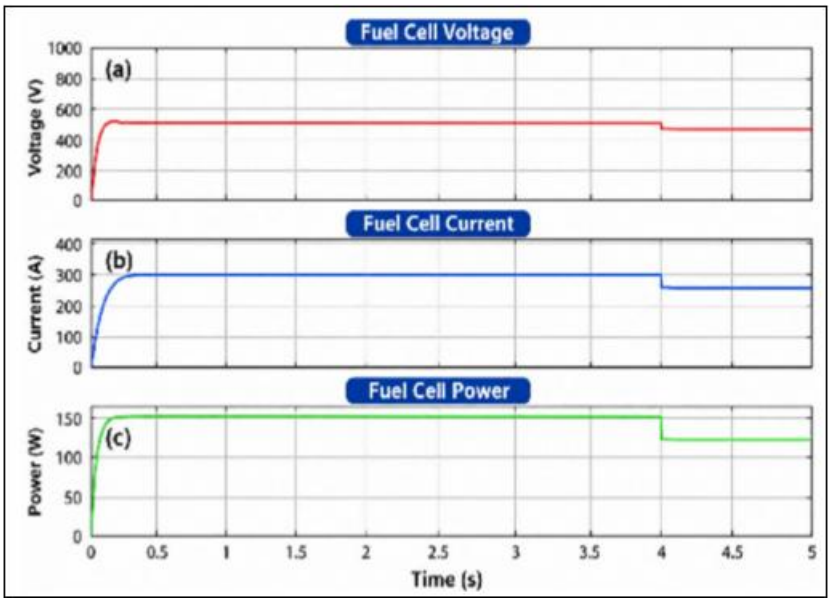


Figure 7: a) Fuel Cell Voltage, b) Fuel Cell Current and c) Fuel Cell Power

DC Link Characteristics

The DC Link Voltage, DC Link Current and DC Link Power characteristics under varying conditions are shown in the Fig.8.

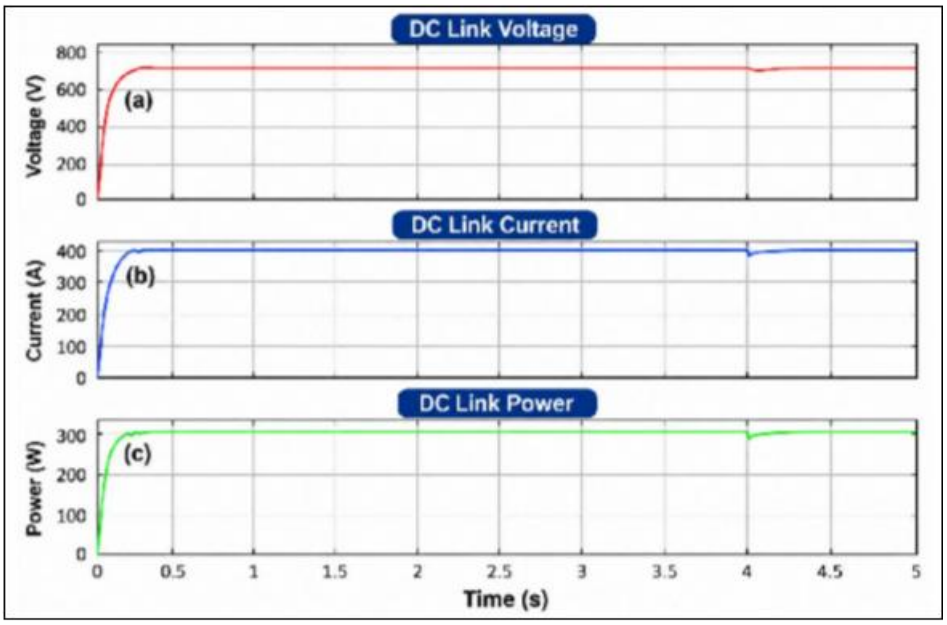


Figure 8: a) DC Link Voltage, b) DC Link Current and c) DC Link Power

Battery output Characteristics

The Battery Output Voltage, Current and Power Characteristics under varying conditions are shown in the Fig.9.

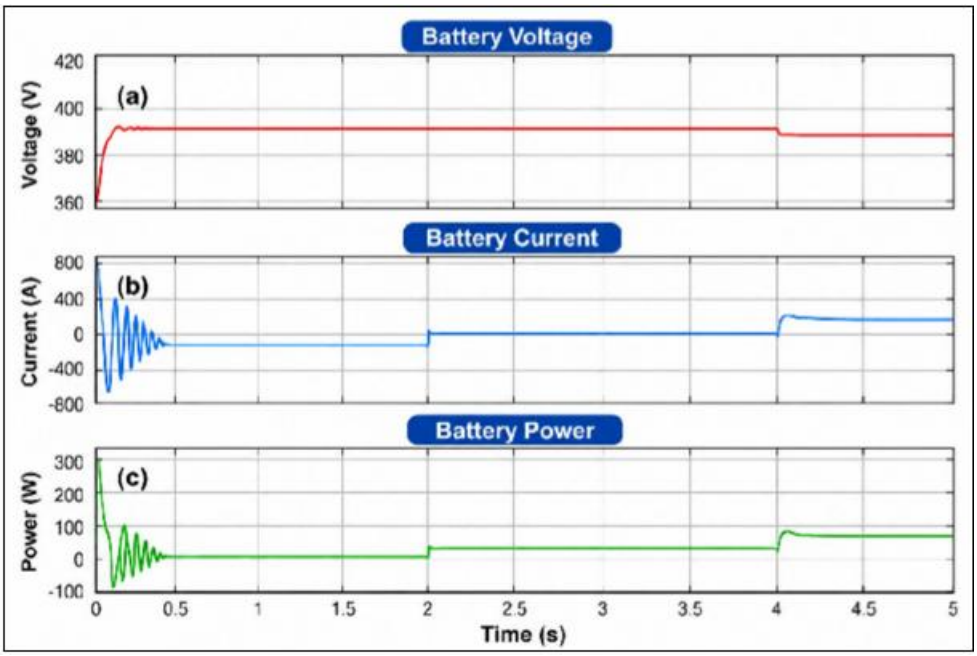


Figure 9: a) Battery Voltage b) Battery Current and c) Battery Power

Comparison of Boost and Interleaved Boost converter under varying conditions

The operational modes of both the conventional boost converter and the suggested dual-phase interleaved boost converter (IBC) were evaluated under varying irradiance, wind speed, and load conditions. The conventional boost converter showed higher input current ripple and slower voltage response, whereas the IBC achieved smoother current sharing between phases, reducing ripple and losses. The IBC maintained a stable DC-link voltage of 700 V compared to 700 ± 5 V for the conventional converter and exhibited faster transient recovery (18 ms vs. 34 ms) with improved efficiency (98% vs. 96.5 %). These results confirm that the interleaved structure enhances voltage regulation, minimizes current stress, and improves overall converter performance under dynamic operating conditions. The proposed Interleaved Boost Converter's enhanced performance contributes directly by enhancing the overall system stability and power quality. By maintaining a steady DC-link voltage with minimal ripple, the inverter receives a more stable input, which reduces modulation stress and improves the sinusoidal quality of the grid-side voltage and current. Consequently, the hybrid system achieves lower total harmonic distortion (THD), better dynamic response, and higher overall efficiency, confirming that the DC-side enhancement through interleaving contributes significantly to superior AC-side performance and seamless grid integration.

6. Inverter and Grid Performance Analysis

The inverter's voltage and current waveforms are depicted in the Fig.10, Fig.11, demonstrating the system's operational characteristics. The grid voltage and grid current waveforms are illustrated in the Fig.12, Fig.13. The THD analysis plots of inverter and grid voltage and current signals are shown in Fig.14 to Fig.17, respectively.

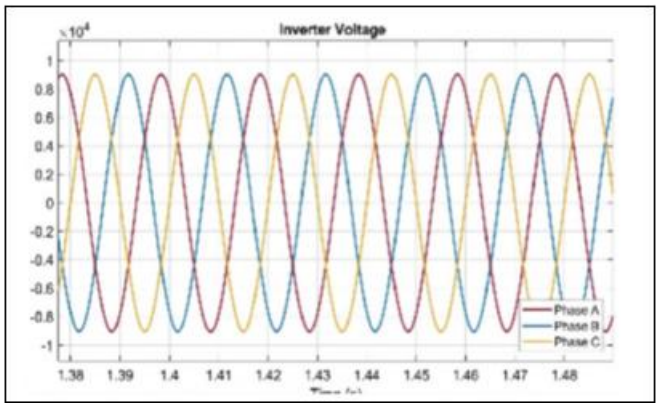


Figure 10: Inverter Voltage

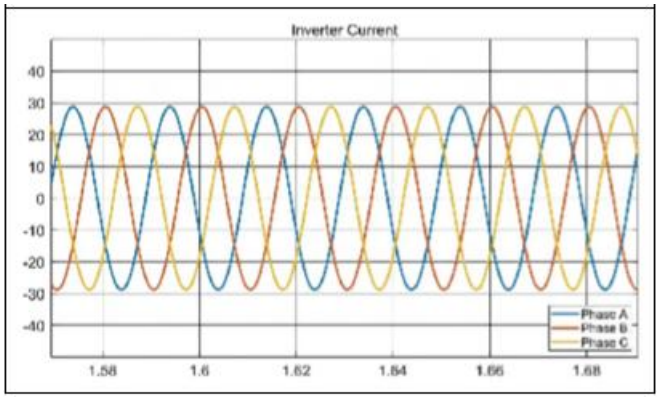


Figure 11: Inverter Current

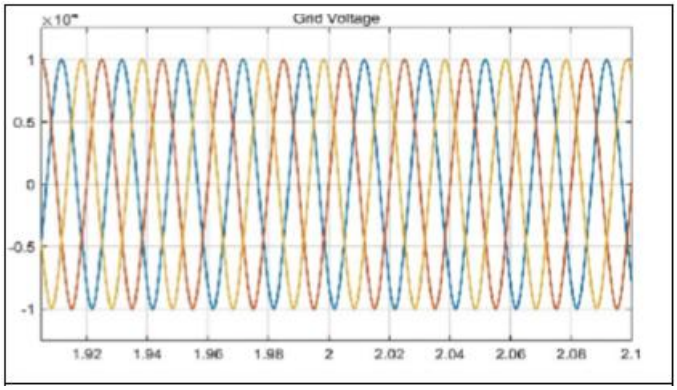


Figure 12: Grid Voltage

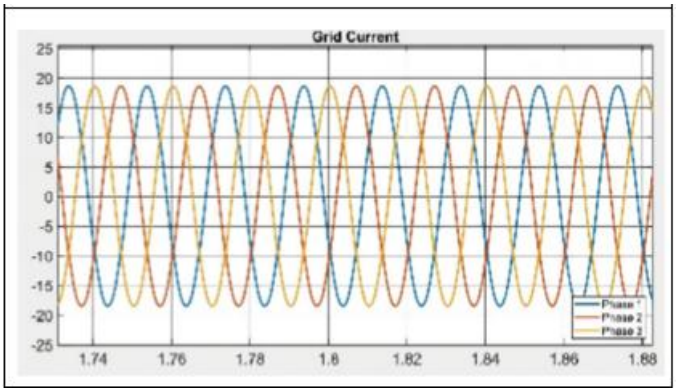


Figure 13: Grid Current

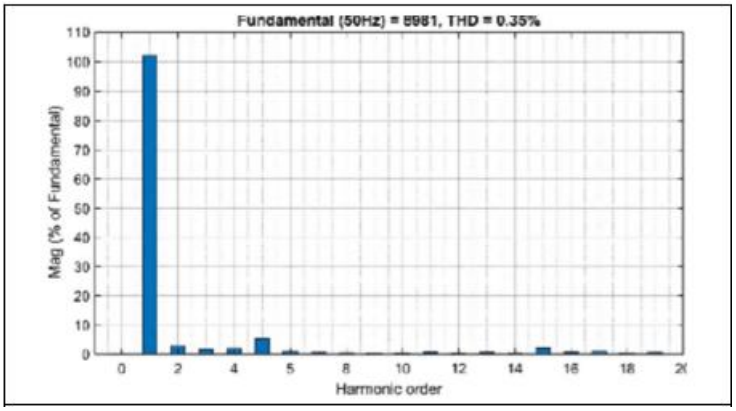


Figure 14: Inverter Voltage THD

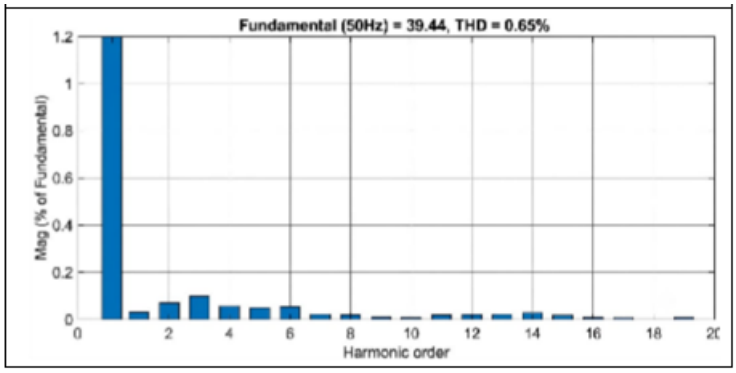


Figure 15: Inverter Current THD

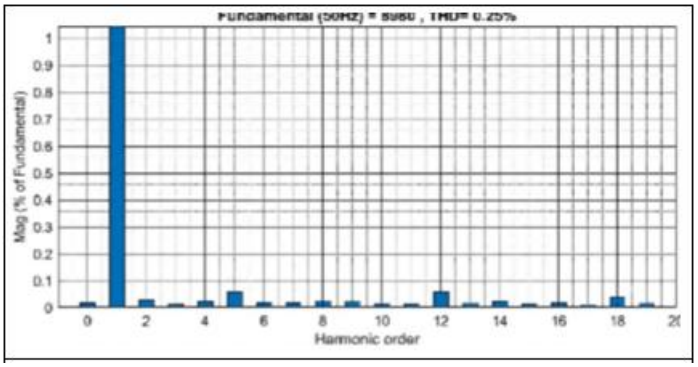


Figure 16: Grid Voltage THD

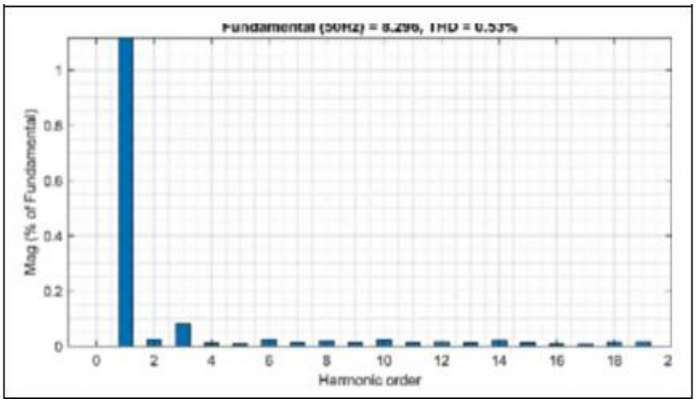


Figure 17: Grid Current THD

The analysis of Total Harmonic Distortion (THD) gave a very clear picture of how much better the GWO based Interleaved Boost Converter (IBC) was over the traditional Boost Converter. For the inverter side, the GWO based IBC system achieved a significant reduction in voltage THD from 2.1% to 0.35% and current THD from 2.3% to 0.65%, indicating improved waveform quality and reduced harmonic content. Similarly, on the grid side, the voltage THD decreased from 2.13% to 0.25%, and the current THD reduced from 2.5% to 0.53%, showing effective mitigation of harmonic distortion and better compliance with IEEE-519 standards. Overall, the results confirm that the GWO based IBC- system enhances power quality, improves inverter and grid performance, and ensures smoother and more stable operation of the grid-tied hybrid renewable energy system.

Operating Condition	Parameter	Boost Converter	IBC	GWO based IBC IBC
Peak Solar–Low Wind Generation	DC-Link Voltage (V)	705 V	700V	700V
	System Output Power (kW)	340	346	348
	BESS Charging Power (kW)	40	46	48
	Efficiency (%)	96.2%	98 %	99%
	Voltage Ripple (%)	3.3 %	0.6 %	0.3%
	Current Ripple (%)	3.1%	1.5%	0.6%
High Solar–Wind Generation	DC-Link Voltage (V)	705 V	700V	700V
	System Output Power (kW)	292	298	300
	BESS Discharge Power (kW)	9	3	2
	Efficiency (%)	96.2 %	98 %	99%
	Voltage Ripple (%)	2.8 %	0.9 %	0.6%

	Current Ripple (%)	3.4%	1.1%	0.8%
Low Solar–High Wind Generation	DC-Link Voltage (V)	695 V	700V	700V
	System Output Power (kW)	270 kW	285	292
	BESS Charging Power (kW)	30 kW	15 kW	8kw
	Efficiency (%)	94.5 %	97.5 %	98%
	Voltage Ripple (%)	4.5 %	1.8 %	0.3%
	Current Ripple (%)	3.5%	1%	0.5%

7. Conclusion

This paper presents a GWO-based MPPT strategy integrated with a dual-phase Interleaved Boost Converter (IBC) for a grid-connected hybrid renewable energy system comprising PV, wind, fuel cell, and battery energy storage sources. The proposed GWO-based optimization enhances maximum power extraction, while the dual-phase IBC reduces current ripple and improves DC-link voltage stability. The bidirectional converter ensures effective battery energy management during variations in renewable generation and load demand. MATLAB/Simulink results demonstrate stable 700 V DC-link operation, improved dynamic performance, and reduced current ripple. The grid-connected inverter with an LCL filter achieves unity power factor and a grid current THD of 0.53%, satisfying IEEE-519 harmonic limits. The proposed configuration offers improved power extraction, system stability, and power quality, making it a promising solution for grid-integrated hybrid renewable energy systems.

References

[1] Q. Hassan, M. A. Khan, and S. A. Malik "A review of hybrid renewable energy systems: Solar and wind integration,", Renewable *and Sustainable Energy Reviews*, vol.169, p.113224,2023.

[2] Z. Sultana, C. H. Basha, M. M. Irfan, and F. Al saif "A novel development of optimized hybrid MPPT controller for fuel cell systems with high voltage transformation ratio DC–DC converter,", *Scientific Reports*, vol.14, Art.no.31536, Dec.2024.

[3] V. Prashanth et al "Implementation of high step-up power converter for fuel cell interfacing in hybrid PV/ wind systems", *Scientific Reports*,2024.

[4] K. Krishnaram, A. R. Murthy, and S. S. Kumar "Performance optimization of interleaved boost converter with hybrid MPPT techniques,", *Scientific Reports*,2024.

[5] S. Nagaraja Rao and A. S. Kumar "Interleaved high-gain boost converter powered by solar energy using hybrid MPP tracking technique,", *Clean Energy*, vol. 6, no. 3, pp. 460–475,2022.

[6] L. Kong "Optimize Photovoltaic MPPT with Improved Snake Algorithm,", *SSRN*,2024.

[7] B.Laxman and A.S.Reddy "A modified particle swarm optimization-based adaptive MPPT for PEMFC systems,", *Energy conversion and Management*,2024.

[8] S. M. Gopal and K. M. Reddy, J. "Design and Control of High Voltage Gain Interleaved Boost Converter for Fuel Cell Based Electric Vehicle Applications," *Electronics, Computer Networking and Applied Mathematics*, vol.3, no.2, pp.9–24,2023.

[9] A. A. Gharah bagh and M. Hosseini "Enhancing efficiency in hybrid solar–wind–battery systems: MPPT improvements and converter interfacing," *Applied Sciences*, vol.14,11710,2024.

[10] P.M. Preethiraj "Design of novel DC–DC interleaved boost converter for renewable applications,", *Journal/ Conference Paper*, 2024.

[11] E. Touti et al "A comprehensive performance analysis of advanced MPPT controllers for PV systems., Sensors, 2024.

[12] S. Vendoti, R. Shankar, and P. C. Gopal "Grid-tied hybrid PV–fuel cell system with energy storage: design and experimental validation,", Scientific *Reports*, 2025.

[13] K. Ishaque, Z. Salam, and G. Lauss ''The performance of perturb and observe and incremental conductance maximum power point tracking method under dynamic weather conditions,'', Appl. *Energy*, vol. 119, pp. 228–236, Apr. 2014,

[14] S. Mateen, M. Amir, A. Haque, and F. I. Bakhsh ''Ultra-fast charging of electric vehicles: A review of power electronics converter, grid stability and optimal battery consideration in multi-energy systems,'', *Sustain. Energy, Grids Netw.*, vol. 35, Sep. 2023.

[15] H. Saleeb, K. Sayed, A. Kassem, and R. Mostafa, ''Control and analysis of bidirectional interleaved hybrid converter with coupled inductors for electric vehicle applications,'' *Electr. Eng.*, vol. 102, no. 1, pp. 195–222, Mar. 2020.

[16] M. V. Naik and P. Samuel, ''Analysis of ripple current, power losses and high efficiency of DC–DC converters for fuel cell power generating systems,'' Renew. *Sustain. Energy Rev.*, vol. 59, pp. 1080–1088, Jun. 2016.

[17] F. K. Faraj and J. Hussain, "Analysis and Comparison of DC–DC Boost Converter and Interleaved DC–DC Boost Converter," Engineering *and Technology Journal*, vol. 38, no. 2, pp. 178–188, 2020.

[18] K. Sakasegawa, T. Shimizu, and Y. Sato, "Comparison of Interleaved Boost Converter and Two-Phase Boost Converter Characteristics for Three-Level Inverters," World *Electric Vehicle Journal*, vol. 14, no. 1, p. 7, 2023.

[19] Selami Balcı and Kadir Sabancı Karamanoglu, "Performance Analysis in a Two-Phase Interleaved DC-DC Boost Converter with Coupled Inductors," *International Journal of Applied Methods in Electronics and Computers*, 2024.

[20] Alik, A. Jusoh & T. Sutikno, "A Review on Perturb and Observe Maximum Power Point Tracking in Photovoltaic System," *TELKOMNIKA*, vol. 13, no. 3, pp. 745-751, Sep. 2015.

[21] Alzahrani, "Interleaved switched-inductor boost converter for photovoltaic energy application," Arabian Journal for Science and Engineering, vol. 48, no. 5, pp. 6419-6430, May 2023.

[22] [22]A.Chauhan and R. P. Saini, "A review on integrated renewable energy system based on solar photovoltaic and fuel cell," *Renewable and Sustainable Energy Reviews*, vol. 38, pp. 99-120, Oct. 2014.
[23] A. Mohamed et al., Distributed energy management of PV–battery–fuel cell hybrid microgrids using adaptive control"*IEEE Transactions on Smart Grid*, 2020.
[24] C. Wang, M.H. Nehrir, H. Gao. "Control of PEMFuel Cell Distributed Generation Systems",IEEE Transactions on Energy Conversion, 2006.
[25] E. Sakasegawa, R. Chishiki, R. Sedutsu, T. Soeda, H. Haga and R. M. Kennel, "Comparison of Interleaved Boost Converter and Two-Phase Boost Converter Characteristics for Three-Level Inverters," *World Electric Vehicle Journal*, vol. 14, no. 1, p. 7, 2023.
[26] F. K. Faraj and J. F. Hussain, "Analysis and comparison of DC–DC boost converter and interleaved DC–DC boost converter," *Engineering and Technology Journal*, vol. 38, no. 5, pp. 622–635, May 2020.
[27] Gharahbagh, A. A. & Hosseini, M., "Enhancing efficiency in hybrid solar–wind–battery systems: MPPT improvements and converter interfacing," *Applied Sciences*, vol. 14(24), 11710, 2024.
[28] Ishaque, K., Salam, Z., & Lauss, G. (2014). "A review of maximum power point tracking techniques of PV system for uniform insolation and partial shading condition." *Renewable and Sustainable Energy Reviews*, 19, 475–488.
[29] Karimulla Syed and Ch. Ravi Kumar Chekka, "Hybrid PSO-HHO Optimal Control for Power Quality Improvement in Autonomous Microgrids," *Journal Européen des Systèmes Automatisés* (JESA), vol. 56, no. 3, pp. 513–517, 2023
[30] K. S. Karimulla Mohammad and C. H. Ravi Kumar, "Power Monitoring in Autonomous DC Micro Grid Connected with SPV Modules," *Journal of Advanced Research in Dynamical and Control Systems*, vol. 12, no. 2, pp. 2142–2148, 2020.
[31] K. H. Hussein, I. Muta, T. Hoshino and M. Osakada, "Maximum photovoltaic power tracking: An algorithm for rapidly changing atmospheric conditions," *IEE Proceedings – Generation, Transmission and Distribution*, vol. 142, no. 1, pp. 59–64, Jan. 1995.
[32] L. Pirashanthiyah, H. N. Edirisinghe, W. M. P. De Silva, S. R. A. Bolonne, V. Logeeshan and C. Wanigasekara, "Design and Analysis of a Three-Phase Interleaved DC–DC Boost Converter with an Energy Storage System for a PV System," *Energies*, vol. 17, no. 1, article 250, 2024.
[33] M. A. Hannan, M. M. Hoque, A. Mohamed and A. Hussain, "Power management strategy for fuel cell–battery–supercapacitor hybrid systems: Issues and challenges," *Applied Energy*, vol. 254, p. 113733, Nov. 2019.
[34] M. V. Naik and P. Samuel, ''Analysis of ripple current, power losses and high efficiency of DC–DC converters for fuel cell power generating systems,'' Renew. *Sustain. Energy Rev.*, vol. 59, pp. 1080–1088, Jun. 2016.
[35] N. Femia, G. Petrone, G. Spagnuolo and M. Vitelli, "Optimization of Perturb and Observe Maximum Power Point Tracking Method," *IEEE Transactions on Power Electronics*, vol. 20, no. 4, pp. 963–973, July 2005.
[36] T. Esram and P. L. Chapman, "Comparison of Photovoltaic Array Maximum Power Point Tracking Techniques," *IEEE Transactions on Energy Conversion*, vol. 22, no. 2, pp. 439–449, June 2007.
[37] K. H. Hussein, I. Muta, T. Hoshino and M. Osakada, "Maximum photovoltaic power tracking: An algorithm for rapidly changing atmospheric conditions," *IEE Proceedings – Generation, Transmission and Distribution*, vol. 142, no. 1, pp. 59–64, Jan. 1995. DOI: 10.1049/ip-gtd:19951577.